

Mechanical and Dry Sliding Wear Behaviour of Al6061/Gr MMCs and its Multi Response Optimization using Hybrid Fuzzy Grey Relational Technique



P. Gangadhara Rao, Pandu R V, K. Meera Saheb

Abstract: An attempt is made to find the mechanical and tribological properties of Al6061/Gr metal matrix composites (MMC) produced using stir casting method. It is important to note that the certain components require high hardness and wear resistance to fulfil the functional requirements, the said properties of the MMCs influenced largely on the condition with which they are produced or treated. Therefore, in the present paper the composites are tested in two stages that is before T6 heat treatment and after T6 heat treatment respectively. The composites are made with Al6061 alloy as matrix and graphite with 3%, 6%, 9% and 12% by wt is considered as reinforcement. Once the composites are prepared, they are examined for their microstructural, mechanical, and tribological properties. Further, a response surface methodology (RSM) has been used to model the wear loss and coefficient of friction for both before and after T6 heat treatment of MMCs. The non-linear regression model obtained is validated both statistically and with the help of experimental test cases. The evidence of wear phenomenon has been observed with the help of Scanning Electron Microscopy (SEM). Further, fuzzy grey relational Technique has been used to determine the multi performance index for the dry sliding wear and friction phenomenon of the developed composite.

Keywords: Response surface methodology, Fuzzy grey relational techniques, Wear loss, Coefficient of friction, MMCs.

I. INTRODUCTION

Now-a-days, Aluminium metal matrix composites (AMMC) are popularly used in engineering applications since they are light in weight and provide better performance in terms of high tensile strength, low density, good thermal and electrical conductivities. It is to be noted that the reliability of AMMC's have been evaluated and proven useful in various fields of engineering, such as aerospace, automotive and defence industries.

They are also used in various structural applications as well as special functional applications due to their custom-made mechanical properties that resulted from the reinforcement of different metals. On the other hand, graphite is considered as the most important constituent for solid lubrication in the alloys and ceramic reinforcement composites. Several researchers had worked on the usage of various carbides, oxides, and graphite as reinforcement materials with various aluminium alloys [1]. Rama Rao and Padmanabhan [2] developed aluminium and boron-carbide composites using stir casting and analyses for microstructural characteristics of the same. The observations show boron carbide powder particles were distributed uniformly throughout the composite due to the stirring action. Ghauri et al. [3] fabricated Al-SiC MMCs after using different volume fractions of SiC. The toughness and hardness were increased due to the existence of SiC particles uniformly in the composite. The mechanical and microstructural characterization of AMMCs reinforced with Nano - MgO particles was studied by Ansary et al. [4]. The observations show that the composite containing 1.5 vol% MgO produces at 850°C develops homogenous microstructure and improved mechanical properties. Further, Alhajeri et al. [5] produced Al6061 MMCs having 10% Al₂O₃ particles by volume using high pressure torsion technique. The results obtained shows considerable enhancement in hardness and the SEM images demonstrate the spreading of Al₂O₃ particles uniformly in the Al6061 metal matrix. Also, this technique brings the strain hardening phenomenon to the composite without considerable recovery. The abrasive wear characteristics, such as coefficient of friction and weight loss of Al-12%SiC reinforced by TiC was investigated by Yigezu et al. [6]. They considered three input parameters namely composition, sliding distance, and load. The results predicted the significant increase in wear resistance characteristics. Baskaran [7] inspected the sliding velocity influence on the wear phenomenon of AA7075/TiC MMCs. The concept of Taguchi's experimental design is applied to observe the wear phenomenon. Further, Rajesh et al. [8] examined the dry sliding wear phenomenon of graphite reinforced with pure aluminium using the statistical modelling to analyze the Wear loss and COF. It was noticed that the COF and wear volume loss were affected by sliding distance and reinforcement respectively.

Revised Manuscript Received on December 30, 2019.

* Correspondence Author

P. Gangadhara Rao*, Department of Mechanical Engineering, Aditya College of Engineering & Technology, Surampalem, Kakinada, AP, India. audibalav@gmail.com

Pandu R V School of Mechanical Sciences, IIT Bhubaneswar, Odisha, India . Email: smartpandu@rediffmail.com

K. Meera Saheb, Department of Mechanical Engineering, JNTUK, Kakinada, AP, India. Email: meer.aec@gmail.com

© The Authors. Published by Blue Eyes Intelligence Engineering and Sciences Publication (BEIESP). This is an [open access](https://creativecommons.org/licenses/by-nc-nd/4.0/) article under the CC-BY-NC-ND license <http://creativecommons.org/licenses/by-nc-nd/4.0/>

Further, Rao et al. [9] experimental work on the wear resistance properties of AA7075/TiC MMC, before and after T6 heat treatment of MMC. It was observed that the after-heat treatment condition the composite resulted better in the mechanical properties and tribological characteristics than that of non-heat treatment condition.

Moreover, Babu Rao [10] investigation on Al7075/SiC MMCs reveals the effect of reinforcement particle dimensions and composition of SiC particles in Al7075 alloy on various wear resistance and mechanical properties respectively. It was observed that the hardness and the UTS of the composites were enhanced with the increase in the content of SiC. In addition to the above works, researchers had also developed certain hybrid metal matrix composites, such as Al6061/SiC/Graphite [11], Al2219/B₄C/MoS₂ [12], Al6061/SiC/TiB₂ [13], Al6061/SiC/ B₄C [14], and studied the mechanical and tribological properties of the composites. Further, few researchers used the concept of RSM to model the dry wear phenomenon of MMCs. Sharma et al. [15] used the statistical methods such as concept of RSM to derive the statistical regression models for the wear phenomenon of Al6082/Graphite MMCs. They considered percentage of reinforcement, load, sliding distance and sliding speed as the inputs for the process and wear loss as the output of the process. In addition to the above research, few researchers used Grey Relational Analysis (GRA) [16-18] and Fuzzy Grey Relational Analysis (FGRA) [19] to perform the multi-objective optimization of wear phenomenon. However, with the best of the authors' knowledge very limited amount of work has been reported in the area of multi-objective optimization of wear phenomenon using FGRT.

In this work an effort is made to produce the Al6061/Graphite MMC through stir casting then examines the mechanical properties and wear behaviour of the prepared composite. While studying the wear behaviour, the concept of RSM has been utilized to perform experiments and to establish the non-linear regression equation for the responses, namely wear loss and coefficient of friction. In the experimentation, the factors, which includes reinforcement percentage, load, sliding distance, and sliding velocity for wear are considered as the input process parameters to generate the statistical modal. ANOVA is used to test the statistical adequacy once the non-linear model is developed. Finally, the adequacy of the model has been verified by experimental test cases. Moreover, microstructural examinations are conducted using SEM to evaluate the wear phenomenon for specimens before and after T6 treatment of AMMCs. Further, multi-objective optimization for the wear and COF has been applied with the help of FGRT.

II. EXPERIMENTAL PROCEDURE

The experimental procedures used in this research are elucidated in the subsequent sub sections.

A. Composites fabrication

In the present research, stir casting (ref. to Fig. 1) route is employed to prepare the aluminium MMCs. Initially, Al6061 aluminium alloy [20] is melted in the crucible and added the designated quantity of reinforcement into it. An appropriate

amount (3% wt. of base metal) of reinforcement (that is, graphite) is preheated to 200°C before injecting into the molten metal. During injecting the reinforcement, an electric stirrer with graphite impeller rotated at 200 RPM is used to stir the molten metal. The stirring process is continued for 10 minutes to obtain uniform distribution of reinforcement particulates. In order to remove the oxides from the melt a degassing agent (that is, hexachloroethane) is added. The liquid melt is transferred to preheated (350°C) die (120 mm x 120 mm x 8 mm) and allowed to solidify in the controlled atmosphere. Figure 2 shows the typical casted specimens produced during the above process. Similar method is adopted to fabricate the remaining compositions with graphite as reinforcement taken in 6% wt, 9% wt and 12% wt and with same Al6061 matrix material.

To study the mechanical and tribological behavior of the AMMCs, before and after T6 treatment condition, a set of fabricated composite specimens are heat treated as well as aged at T6 condition. During the T6 heat treatment process, the composite specimens are solutionized at a temperature of 538°C for one hour then after water quenched, further the composite specimens are aged at temperature 171°C for ten hours and then quenched in air media.

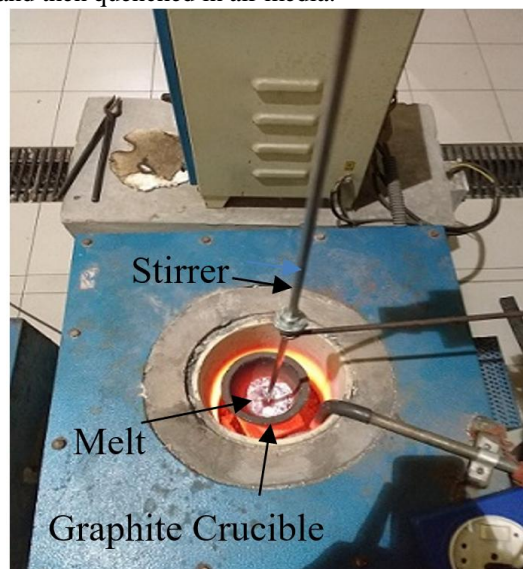


Fig. 1. Diagram showing the details of pit furnace.



Fig. 2. Cast specimens produced from pit furnace.

B. Hardness test

The representative samples for hardness test are cut from the fabricated AMMCs.

The Brinell's hardness testing machine (make: Indentec) shown in Fig. 3, is utilized to conduct the hardness test as per IS 1501:2002 ASTM standards [21]. A steel ball with a diameter of 5 mm is used as indenter and applied a load of 250 Kgf for 25s.



Fig. 3. Details of Brinell's hardness testing machine.



Fig. 4. Details of the indentations at three locations of ball in hardness test specimens.

It is important to note that the hardness of the sample is measured at three distinct locations (ref. to fig. 4) to avoid the measurement uncertainties and the average of the three readings is considered as the hardness of the sample. The hardness test is conducted on specimens before and after T6 heat-treatment specimens.

C. Tensile test

The schematic diagram showing the universal testing machine (model: TUV-C-200) is shown in Fig. 5. The tensile tests are conducted with the adopted procedure of ASTM B 557 [22] standards. The tensile testing specimens (ref. to Fig. 6) with a gauge length of 25 mm in length are cut on the WEDM (model: Excetek-EX40) and the specimens are prepared for testing before and after T6 treatment.



Fig. 5. Universal testing machine.



Fig. 6. Specimens of tensile test.

D. Modelling of wear phenomenon using RSM

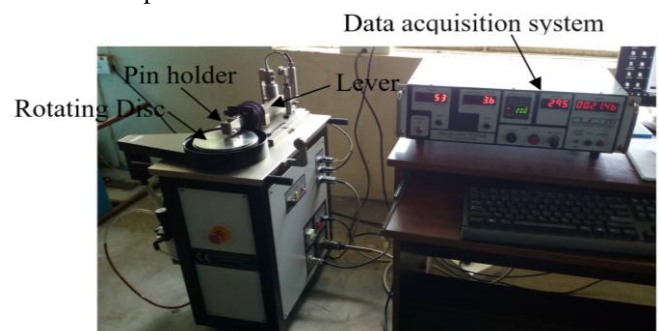
Once the mechanical properties are evaluated, an attempt is made to check the WL and COF with the help of RSM. The wear test is performed on a wear test apparatus model: TR-20LE-PHM400 shown in Fig. 7. The specimens for wear test are prepared with 6 mm circular cross section and are polished carefully at the sliding end (ref. to Fig.7b) and then the sliding end of the pin and surface of the disc are cleaned properly using acetone.

The number of experiments required to conduct the wear test are decided with the help of central composite design of experiments. The process variables such as load, reinforcement percentage, sliding distance and sliding speed are considered as the input parameters, and the two output parameters such as WL and COF are considered as the responses of process. The input process parameters range used in this study are given in Table 1.

Table 1: Represents the input variables and their ranges.

S. no	Name of factors	Notation	Lower Range (-1)	Upper Range (+1)
I	%Graphite composition	%Gr	3.00	9.00
II	Applied Load	L	10.00	30.00
III	Sliding distance (m)	D	500.00	2500.00
IV	Sliding velocity (m/s)	V	1.00	3.00

The experiments are designed and analysed using the Minitab 17 statistical design software tool. Once the experiments are conducted, the WL and COF are measured as responses to check the dry sliding wear phenomenon of Al6061/Gr composites.



(a)



(b)

Fig. 7. The wear test: (a) Dry sliding wear experimentation setup (b) Specimens.

E. Multi-objective optimization using Hybrid Fuzzy Grey Relational Technique (FGRT)

The present study also aimed to determine the multi-performance characteristics of the wear process. To achieve this, a hybrid fuzzy GRT algorithm is applied, and the flow chart of this algorithm is shown in Fig. 8. The procedure employed for the determination of GRC is same as the procedure used in the conventional GRA [23]. The arithmetic mean of various GRCs is considered as the grey relational grade (GRG) in the GRT approach, whereas in the proposed method (that is, FGRT), Mamdani-based Fuzzy Logic Controller (FLC) is used in the estimation of GRGs. [24].

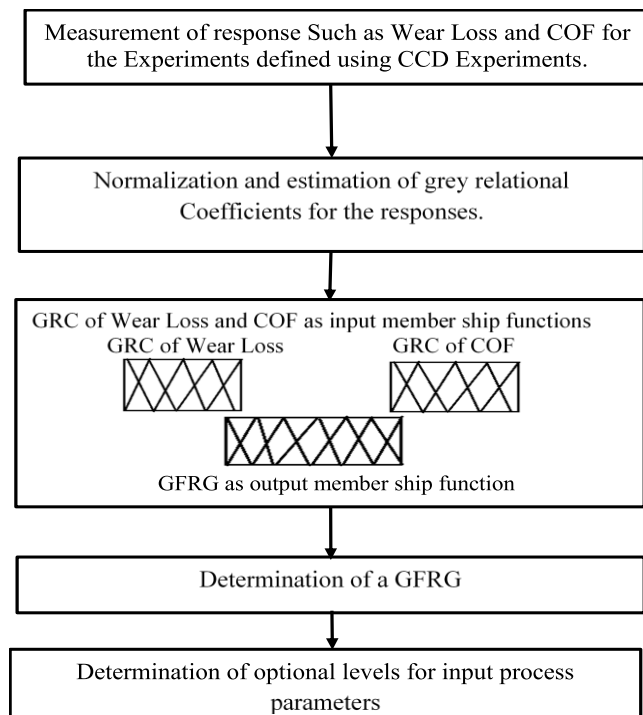


Fig 8: The flow chart shows various steps involved in FGRT algorithm.

In the present work, GRCs of output responses that is WL and COF are considered as inputs. The fuzzification was done using the triangular membership functions which are shown in figure 9. To estimate the grey fuzzy relational grade (GFRG) an interference engine is generated using if-then rules between the individual grey relational coefficients. The optimal input parameters are determined from the resulted GFRG values.

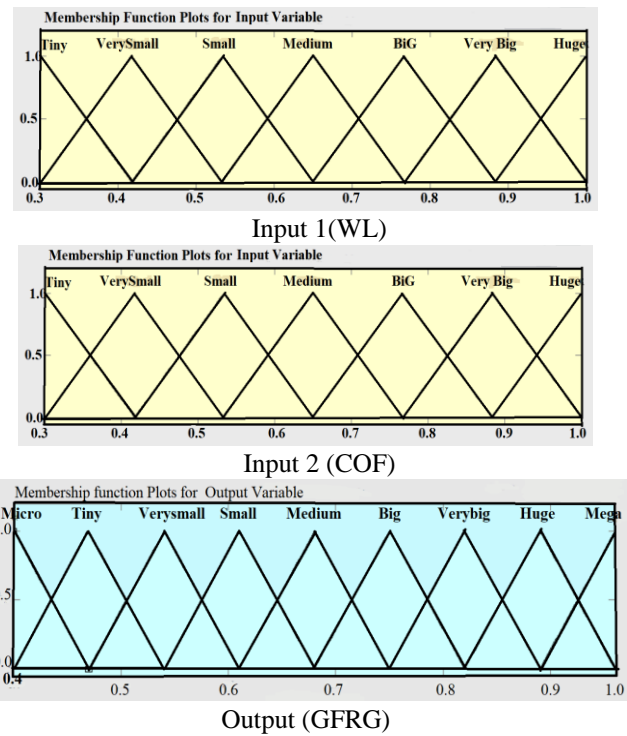


Fig. 9. Schematic diagram showing the triangular membership function distribution of input variables WL, COF, and output responses (GFRG).

III. RESULT AND DISCUSSION

A. SEM examination

SEM analysis is performed to examine the microstructural details of both before and after T6 heat treatment of AMMCs and are shown in Fig. 10 and Fig. 11, respectively. The micrographs exhibited a reasonably uniform dispersion of

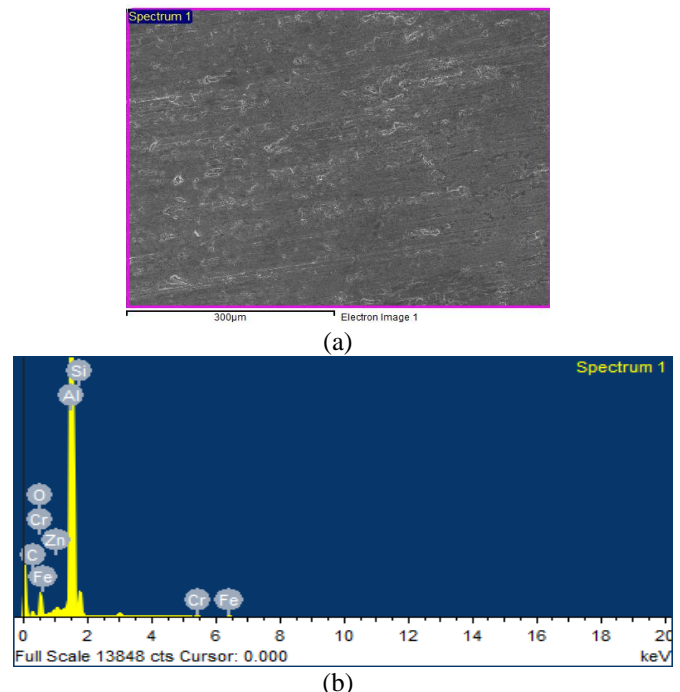
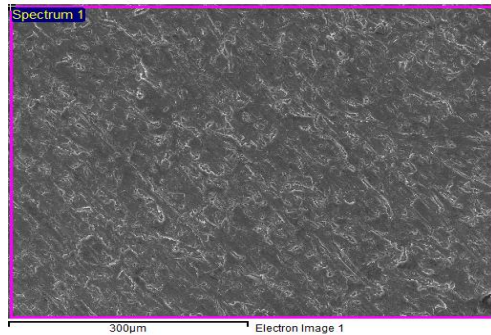
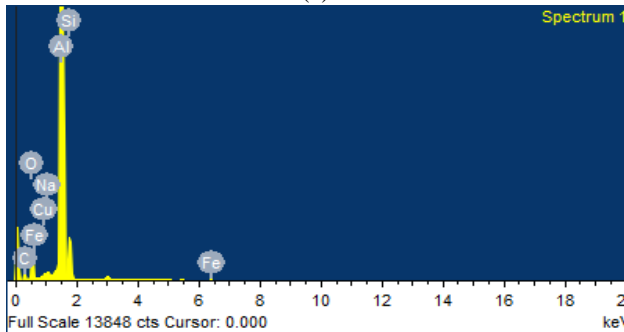


Fig. 10. SEM-EDX analysis of AMMCs. (a) SEM Image and (b) EDX of 3% Gr before-T6 treatment of AMMCs.

graphite and matrix reinforcement interfacial bonding. It has also been observed that the reaction products are also formed due to the interfacial reaction. The analysis was conducted at Kelvin Labs, Hyderabad, Telangana. From figures 10 and 11, the following conclusions are drawn: i) Observed uniform dispersion of reinforcement without forming agglomerations, ii) Enhancement in the interfacial bonds with increase in the reinforcement percentage, iii) Formation of agglomerations with increase in the reinforcement percentage from 9% to 12% of reinforcement.



(a)



(b)

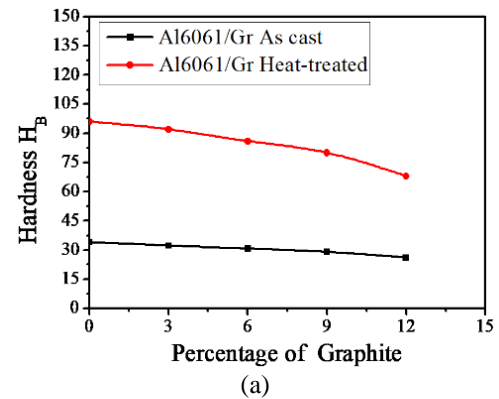
Fig. 11 SEM-EDX analysis of AMMCs. (a) SEM and (b) EDX of 9% Gr before-T6 treatment of AMMCs.

B. Hardness

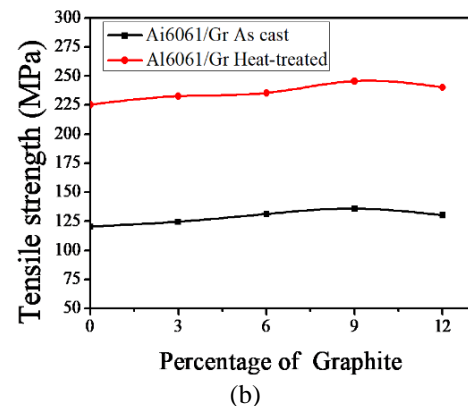
The results of Brinell's hardness test for both conditions that is before and after T6 treatment. In the graphs before heat treatment condition mentioned as as-cast and after treatment mentioned as heat-treated respectively. The figure 12 shows these hardness graphs of Al6061/Gr MMCs. In the figure 12a, it is observed that the increase in the percentage of graphite (that is, reinforcement) resulted in the reduction of hardness value of the composite. This might have happened because the density of graphite is low when compared with the matrix material and float in the molten pool during melting and resulted in weak interfacial bonding among the reinforcement and matrix. This phenomenon is more dominating when there is an increase in the weight percentage of reinforcement and leads to decrease in the hardness of the composite. The obtained results correlate with the results available in the literature.

Figures 12b and 12c show the effect of graphite (that is, reinforcement) on the strength and percentage elongation, respectively for both before and after T6 conditions of Al6061/Gr composites. It has been observed that the tensile strength of the composite is seen to decrease initially from pure Al alloy to 3% reinforcement. Further, there is an increase in this value up to 9% wt of reinforcement and then decreases with the increase in the value of reinforcement. This

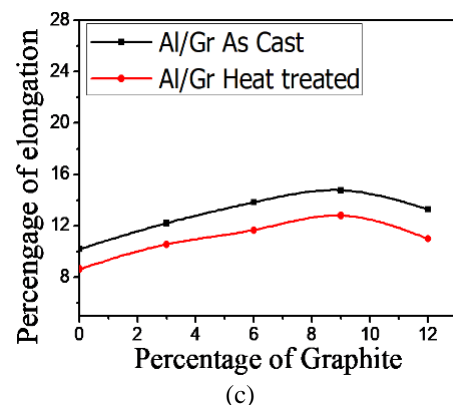
is also true with the heat treated AMMC. It may be due to the reason that at the early stage, low percentage of reinforcement may act like an impurity rather than reinforcement. When the percentage weight of graphite increases, its reinforcement effect is more and resulted in improved tensile strength. Further, when the percentage of reinforcement reaches 12%, then graphite enforces its properties, such as low tensile strength and percentage elongation on the composite and resulted in lowering the same. This explanation also holds good for percentage elongation. It has also been observed that the values in heat-treated condition are generally higher than the before T6 treatment condition values of the same composition due to the homogeneous distribution of matrix and reinforcement in the composite.



(a)



(b)



(c)

Fig.12. properties before-T6 treatment and after-T6 heat treatment of AMMCs (a) Hardness - percentage of graphite (b) Tensile strength - percentage of graphite (c) Percentage of elongation - percentage of graphite

Mechanical and Dry Sliding Wear Behaviour of Al6061/Gr MMCs and its Multi Response Optimization using Hybrid Fuzzy Grey Relational Technique

C. Wear model by RSM

The experimental data collected from the wear test which is established on the concept of central composite design for both before T6 treatment and after T6 heat treatment conditions are given in Table 2. The non-linear regression equations that represent the WL and COF in terms of input process parameters for both the before T6 treatment of Al6061/Gr MMCs and after T6 treatment of Al6061/Gr MMCs are given in Eqns. (1), (2), (3), and (4) respectively.

$$WL_{\text{before-T6}} = 0.1451 + 0.08839\%Gr - 0.12991\%L + 0.000379\%D + 0.4877\%V - 0.007919\%Gr\%Gr + 0.003314\%L\%L - 0.11842\%V\%V + 0.000048\%Gr\%L + 0.000104\%Gr\%V + 0.000019\%L\%V. \quad (1)$$

$$COF_{\text{before-T6}} = 0.6369 + 0.1013\%Gr - 0.03801\%L + 0.000072\%D - 0.2241\%V - 0.00524\%Gr\%Gr + 0.000566$$

$$\%L\%L + 0.0197\%V\%V - 0.000975\%Gr\%L - 0.000006\%Gr\%D - 0.00156\%Gr\%V + 0.000002\%L\%D + 0.005371\%L\%V + 0.000028\%D\%V.$$

(2)

$$WL_{\text{after-T6}} = 0.1711 - 0.2608\%Gr + 0.01594\%L + 0.000182\%D + 0.3432\%V + 0.021651\%Gr\%Gr - 0.000370\%L\%L - 0.08349\%V\%V + 0.000013\%Gr\%L - 0.000083\%Gr\%V - 0.000012\%L\%V + 0.000010\%D\%V. \quad (3)$$

$$COF_{\text{after-T6}} = 0.7696 + 0.0359\%Gr - 0.05319\%L + 0.000104\%D - 0.1524\%V - 0.000060\%Gr\%Gr + 0.001177\%L\%L + 0.00566\%V\%V - 0.001145\%Gr\%L - 0.000006\%Gr\%D + 0.00168\%Gr\%V - 0.000001\%L\%D + 0.004962\%L\%V + 0.000002\%D\%V. \quad (4)$$

Table 2: Experimental results for before and after T6 heat treated AMMCs

S no	%Gr	Load	Sliding distance	Sliding velocity	Before-T6		After-T6	
					WL	COF	WL	COF
1	3	10	500	1	0.076	0.499	0.022	0.406
2	9	10	500	1	0.037	0.632	0.012	0.562
3	3	30	500	1	0.131	0.246	0.043	0.322
4	9	30	500	1	0.103	0.269	0.035	0.314
5	3	10	2500	1	0.125	0.435	0.061	0.497
6	9	10	2500	1	0.092	0.541	0.051	0.565
7	3	30	2500	1	0.182	0.304	0.082	0.361
8	9	30	2500	1	0.153	0.228	0.073	0.273
9	3	10	500	3	0.105	0.311	0.053	0.282
10	9	10	500	3	0.071	0.444	0.044	0.42
11	3	30	500	3	0.163	0.294	0.072	0.36
12	9	30	500	3	0.133	0.306	0.064	0.383
13	3	10	2500	3	0.156	0.423	0.131	0.355
14	9	10	2500	3	0.124	0.433	0.118	0.436
15	3	30	2500	3	0.215	0.427	0.153	0.409
16	9	30	2500	3	0.187	0.383	0.142	0.376
17	6	20	1500	2	0.107	0.366	0.045	0.264
18	6	20	1500	2	0.110	0.414	0.055	0.293
19	6	20	1500	2	0.100	0.379	0.05	0.285
20	6	20	1500	2	0.106	0.413	0.075	0.3
21	3	20	1500	2	0.104	0.202	0.293	0.176
22	9	20	1500	2	0.077	0.246	0.3075	0.208
23	6	10	1500	2	0.466	0.404	0.044	0.343
24	6	30	1500	2	0.520	0.252	0.093	0.277
25	6	20	500	2	0.015	0.221	0.0307	0.177
26	6	20	2500	2	0.072	0.246	0.065	0.179
27	6	20	1500	1	0.030	0.271	0.013	0.209
28	6	20	1500	3	0.055	0.311	0.031	0.188
29	6	20	1500	2	0.154	0.287	0.099	0.211
30	6	20	1500	2	0.154	0.281	0.102	0.188

The statistical adequacy of the developed non-linear equations is examined by conducting the ANOVA test. The results of ANOVA related to the WL during the wear test of before T6 treatment Al6061/Gr are tabulated in Table 3.

ANOVA results show that except the interaction terms, all other terms are having a notable contribution to the response WL as their p-values seems to be less than 0.050.

Similar tests have also been conducted for the COF of before T6 treatment. Further, these tests are continued for the COF and WL of after T6 treatment condition of Al6061/Gr MMC. It is noticed that the (COF) linear and square terms of sliding velocity and the interaction term of graphite percentage and sliding velocity are seen to be insignificant for before-T6 AMMCs. Similar to the WL of before T6 treatment of MMC, the effect of all interaction terms is found to be insignificant

on the WL of after T6 treatment of MMC. Moreover, the square terms of sliding velocity, load, and the interaction terms of graphite percentage and sliding distance with sliding velocity seems to be insignificant on the COF of after T6 treatment of MMC. Further, the response plots for the WL of after T6 treatment of Al6061/Gr MMC are shown in Fig. 13. The observations that are drawn

Table 3: the results of ANOVA for WL of before T6 treatment Al6061/Gr MMC

Source of variation	Degree of freedom	Adj. Sum of Squares	Adj. Mean Sum of Squares	F-Value	P-Value
Regression model	15	0.3071090	0.0204740	48.040	0.0000
Blocks	1	0.0562410	0.0562410	131.970	0.0000
Linear-terms	4	0.119954	0.029988	70.37	0.000
Percentage of Graphite	1	0.006441	0.006441	15.11	0.002
Applied load(N)	1	0.110878	0.110878	260.18	0.000
Sliding Distance	1	0.002171	0.002171	5.09	0.041
Sliding Velocity	1	0.000463	0.000463	1.09	0.315
Square-terms	4	0.014715	0.003679	8.63	0.001
(% Graphite) * (% Graphite)	1	0.005641	0.005641	13.24	0.003
(Applied load) *(Applied load)	1	0.008135	0.008135	19.09	0.001
(Sliding Distance) *(Sliding Distance)	1	0.003645	0.003645	8.55	0.011
(Sliding Velocity) *(Sliding Velocity)	1	0.000986	0.000986	2.31	0.150
Two-Way Interaction terms	6	0.083532	0.013922	32.67	0.000
(% Graphite) *(Applied Load)	1	0.013683	0.013683	32.11	0.000
(% Graphite) *(Sliding Distance)	1	0.005828	0.005828	13.68	0.002
(% Graphite) *(Sliding Velocity)	1	0.000351	0.000351	0.82	0.380
(Applied load(N)) *(Sliding Distance)	1	0.004885	0.004885	11.46	0.004
(Applied load(N)) *(Sliding Velocity)	1	0.046157	0.046157	108.31	0.000
(Sliding Distance) *(Sliding Velocity)	1	0.012628	0.012628	29.63	0.000
Source of variation	R-Sq	R-Sq(Adj)	R-Sq-(Pred.)		
0.0206435	98.09%	96.05%	89.70%		

from the surface plots are as follows: Fig. 13(a) shows that the wear loss decreases with the increase in the percentage of reinforcement. This may be due to the self-lubricating nature of the graphite when compared with the Al6061 alloy matrix that leads to the reduction in the wear loss. Further, it is observed that with increase in load the wear loss increases.

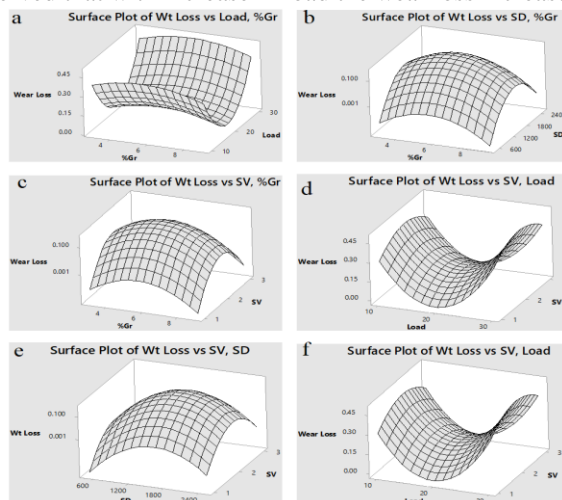


Fig 13: surface plots for variation of WL during wear test of before T6 treatment of Al6061/Gr MMCs.

This may be due to the formation of the softened surface due to the heating of the contact surface with the application of

load. From Fig. 13(b), it can be seen that the increase in the graphite percentage resulted in the wear loss reduction. This is due to the same reason as the one explained above. Moreover, the increase in the value of sliding distance increases the wear loss. This might have happened due to the prolonged sliding contact with the application of external load between two surfaces.

The wear loss has shown a non-linear decrease with increase in reinforcement percentage and shows an increasing trend with the increasing value of sliding velocity (ref. to Fig. 13 (c)). This might be due to the softened surface formed due to the heating at the contact surface with the application of sliding velocity and load. The response plots for sliding velocity and sliding distance with the variation in load is shown in Fig. 13 (d) and (e), respectively. In both cases, the wear loss increases with the increasing values of sliding velocity and sliding distance, which is also evident from Fig. 13 (f). These observations are in-line with the results available in the literature. Moreover, the coefficients of correlation values of COF and WL for before T6 treatment Al6061/Gr MMC and after T6 treatment Al6061/Gr MMC are seen to be equal to {99.93, 98.09} and {98.66, 99.22}, respectively.

Mechanical and Dry Sliding Wear Behaviour of Al6061/Gr MMCs and its Multi Response Optimization using Hybrid Fuzzy Grey Relational Technique

This shows that the non-linear regression models developed to represent the wear process for before T6 treatment AMMCs and after T6 treatment AMMCs are very closely representing the physical system. Further, confirmation experiments are conducted to examine the prediction accuracy of the non-linear regression equations developed using the central composite design of experiments. Fig. 14 shows the variation of percentage error for the experimental test cases for both the before and after T6 heat treatment of

AMMCs. The percentage error values range of WL and COF for before and after T6 heat treatment of Al6061/Gr MMCs are found to lie in the range of $\{(-11.91 \text{ to } +12.16), (-8.66 \text{ to } +11.46)\}$ and $\{(-9.01 \text{ to } +4.42), (-3.22 \text{ to } +6.91)\}$, respectively. Therefore, it can be concluded that the non-linear regression equations derived above correlated the wear process of Al6061/Gr MMCs with a reasonably good degree of approximation.

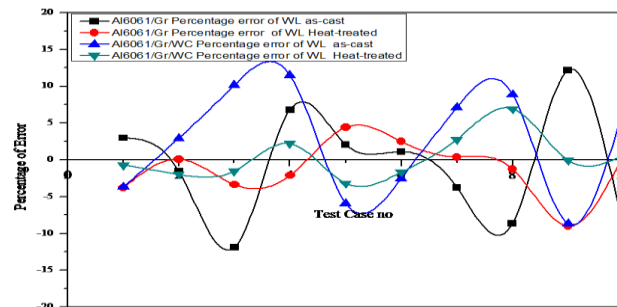


Fig. 14. Graph showing the comparison of percentage deviation of COF and WL before and after T6 heat treatment of Al6061/Gr MMCs.

Table 4: displays the normalized values, deviation sequence and GRCs of before and after T6 heat treated Al6061/Gr MMCs

S no	Al6061/Gr as-cast							Al6061/Gr heat-treated						
	Normalized Values		Deviation Values		GRC		GFRG	Normalized Values		Deviation Values		GRC		GFRG
	WL	COF	WL	COF	WL	COF		WL	COF	WL	COF	WL	COF	
1	0.879	0.309	0.121	0.691	0.805	0.420	0.580	0.966	0.409	0.034	0.591	0.937	0.458	0.710
2	0.956	0.000	0.044	1.000	0.920	0.333	0.610	1.000	0.008	0.000	0.992	1.000	0.335	0.670
3	0.770	0.898	0.230	0.102	0.685	0.830	0.726	0.895	0.625	0.105	0.375	0.827	0.571	0.700
4	0.826	0.844	0.174	0.156	0.742	0.762	0.715	0.922	0.645	0.078	0.355	0.865	0.585	0.730
5	0.782	0.458	0.218	0.542	0.697	0.480	0.575	0.834	0.175	0.166	0.825	0.751	0.377	0.632
6	0.848	0.212	0.152	0.788	0.766	0.388	0.581	0.868	0.000	0.132	1.000	0.791	0.333	0.637
7	0.669	0.763	0.331	0.237	0.602	0.678	0.660	0.763	0.524	0.237	0.476	0.679	0.513	0.674
8	0.727	0.940	0.273	0.060	0.647	0.892	0.750	0.794	0.751	0.206	0.249	0.708	0.667	0.732
9	0.822	0.747	0.178	0.253	0.737	0.664	0.693	0.861	0.728	0.139	0.272	0.783	0.647	0.723
10	0.889	0.437	0.111	0.563	0.818	0.470	0.558	0.892	0.373	0.108	0.627	0.822	0.444	0.675
11	0.707	0.786	0.293	0.214	0.630	0.700	0.681	0.797	0.527	0.203	0.473	0.711	0.514	0.676
12	0.766	0.758	0.234	0.242	0.682	0.674	0.697	0.824	0.468	0.176	0.532	0.740	0.484	0.663
13	0.721	0.486	0.279	0.514	0.642	0.493	0.554	0.597	0.540	0.403	0.460	0.554	0.521	0.569
14	0.784	0.463	0.216	0.537	0.698	0.482	0.575	0.641	0.332	0.359	0.668	0.582	0.428	0.515
15	0.604	0.477	0.396	0.523	0.558	0.489	0.505	0.523	0.401	0.477	0.599	0.512	0.455	0.512
16	0.659	0.579	0.341	0.421	0.595	0.543	0.533	0.560	0.486	0.440	0.514	0.532	0.493	0.513
17	0.818	0.619	0.182	0.381	0.733	0.567	0.601	0.888	0.774	0.112	0.226	0.817	0.688	0.744
18	0.812	0.507	0.188	0.493	0.727	0.504	0.575	0.854	0.699	0.146	0.301	0.775	0.624	0.715
19	0.832	0.588	0.168	0.412	0.748	0.548	0.617	0.871	0.720	0.129	0.280	0.795	0.641	0.721
20	0.820	0.509	0.180	0.491	0.735	0.505	0.577	0.787	0.681	0.213	0.319	0.701	0.611	0.701
21	0.824	1.000	0.176	0.000	0.739	1.000	0.890	0.049	1.000	0.951	0.000	0.345	1.000	0.720
22	0.878	0.897	0.122	0.103	0.804	0.830	0.820	0.000	0.918	1.000	0.082	0.333	0.859	0.600
23	0.107	0.530	0.893	0.470	0.359	0.516	0.423	0.892	0.571	0.108	0.429	0.822	0.538	0.698
24	0.000	0.884	1.000	0.116	0.333	0.811	0.540	0.726	0.740	0.274	0.260	0.646	0.658	0.669
25	1.000	0.956	0.000	0.044	1.000	0.919	0.890	0.937	0.997	0.063	0.003	0.888	0.995	0.900
26	0.888	0.898	0.112	0.102	0.816	0.830	0.820	0.821	0.992	0.179	0.008	0.736	0.985	0.841
27	0.970	0.840	0.030	0.160	0.944	0.757	0.810	0.997	0.915	0.003	0.085	0.993	0.855	0.922
28	0.921	0.747	0.079	0.253	0.863	0.664	0.738	0.936	0.969	0.064	0.031	0.886	0.942	0.922
29	0.726	0.802	0.274	0.198	0.646	0.717	0.674	0.706	0.910	0.294	0.090	0.629	0.847	0.740
30	0.725	0.816	0.275	0.184	0.645	0.731	0.696	0.695	0.969	0.305	0.031	0.621	0.942	0.851

D. Fuzzy GRA

In the present paper, the GRCs of COF and WL, which are used as inputs to the FLC are calculated from GRA procedure. Here the deviation sequence, normalized values, and GRCs of before and after T6 heat treatment of MMCs obtained are tabulated in Table 4.

Once the GRCs for WL and COF are obtained, then the fuzzy rule base (Ref. to Fig. 15) is constructed between the inputs and output of the wear process. For each experiment the GRG will be predicted once the fuzzy rule base is constructed and by providing the GRCs of COF and WL as inputs to FLC. The fuzzy predicted values are converted to multiperformance characteristic known as GFRG by Defuzzifier. The GFRG values are tabulated in Table 4. Once the GFRG values are obtained, the response table for grey fuzzy reasoning grade (ref. to Table 5) will be calculated after taking the average GFRG of each level for the corresponding input process parameters. Observing the data presented in Table 5, it can be concluded that levels of the parameters A2, B2, C1, and D2 are carries a higher average FGRG values compared with the other values present in the table. Therefore, it can be concluded that the sequence A2-B2-C1-D2 is found to be the optimal combination of input parameters for the wear test of Al6061/Gr MMC before T6 treatment. For the after T6 heat treatment of AMMCs the obtained combination noted as A2-B2-C2-D2 respectively. Further, the impact of a particular input variable on the wear process for both before and after T6 heat treatment of AMMCs are determined and tabulated in Table 5 and Table 6, respectively. Further, the impact of a particular input variable on the wear process for both before and after T6 heat treatment of AMMCs are determined and tabulated in Table 5 and Table 6, respectively. The impact of a particular variable on the response is decided based on the difference between the maximum and minimum values of average GFRG values of that particular input parameter. Therefore, from Tables 5 and 6, load and percentage of graphite seems to have more influence on the responses when compared with the other input parameters of Al6061/Gr MMCs before and after T6 heat treatment. Further, confirmation experiments have been conducted for the optimum conditions of before-T6 treatment. Further,

Table 5 optimal input parameters for GFRG of Al6061/Gr before-T6 treatment composite.

Level	%Gr	Load	Sliding Distance	Sliding Velocity
I	0.6515 6 0.6634	0.5721 1 0.7256		
II			0.66342	0.67692
III	0.6487 8	0.6452 2	0.61700	0.61489
Max -Min	0.0146 4	0.1535 6	0.06633	0.06203
Rank	2	1	3	4

Table 6 optimal input parameters for GFRG of Al6061/Gr after-T6 treatment composite.

Level	%Gr	Load	Sliding Distance	Sliding Velocity
I	0.6540 0 0.7853	0.64656	0.71189	0.70744
II		0.77975	0.74858	0.74000
III	0.6338 9	0.72378	0.62500	0.72311
Max -Min	0.1514 4	0.13319	0.12358	0.03256
Rank	1	2	3	4

confirmation experiments have been conducted for the optimum conditions of before T6 treatment (A2-B2-C1-D2) and after T6 treatment (A2-B2-C2-D2) Al6061/Gr MMCs. Figure 16 (a) and Figure 16 (b) show the worn-out surfaces' micrographs of before T6 treatment AMMCs and T6 treatment AMMCs respectively. From Figs. 16 (a) and (b), it has been observed that the fine scratches are observed in the sliding direction of the before T6 treatment condition become larger distinct grooves in the direction of sliding in case of after T6 treatment specimens. This might happen due to the homogenization of the crystal grain structures in the case of heat-treated Al6061/Gr MMCs. These results are in line with the data available in the literature.



(a)



(b)

Fig 16: SEM images of the worn-out pin at optimum conditions, (a) before T6 treatment and (b) after T6 treatment Al6061/Gr MMCs.

IV. CONCLUSION

In this work, an attempt is made to develop and study the microstructural and mechanical behaviour of Al6061/Gr MMCs produced using stir casting route. Further, an attempt is also made to formulate a non-linear regression model to predict before T6 treatment and T6 treatment MMCs wear behaviour. The microstructural observation with SEM revealed homogeneous distribution of graphite (that is, reinforcement) in composites.

Further, the wear modelling of Al6061/Gr composites for both the before T6 treatment and after conditions show that all the four input variables, namely reinforcement percentage, sliding distance, load, and sliding velocity have significant contribution on the WL and COF. Moreover, a hybrid fuzzy GRA approach is developed to determine the optimal input process parameters that optimize the COF and WL of before T6 treatment and after T6 treatment Al6061/Gr MMCs. The micrographs of validation experiments show evidence of uniform wear in the heat-treated condition conclusion section is not required.

So, it is concluded that the Al6061/GrT6 MMCs better than the Al6061T6 alloy in tribological as well as mechanical properties.

REFERENCES

1. G.B. Veeresh Kumar, C.S.P. Rao, N. Selvaraj, and M.S. Bhagyashekar, Studies on Al6061-SiC and Al7075-Al₂O₃ metal matrix composites, Journal of Minerals and Materials Characterization & Engineering, Vol. 9, No. 1, pp. 43-55, 2010.
2. S. Rama Rao and G. Padmanabhan, Fabrication and mechanical properties of aluminium- boron carbide composites, International Journal of Materials and Biomaterials Application, Vol. 2, No. 3, pp. 15-18, 2012.
3. K.M. Ghauri, L. Ali, A. Ahmed, R. Ahmed, K.M. Din, I.A. Chaudhary, and R.A. Karim, Synthesis and characterization of Al/SiC composite made by stir casting method, Pakistan Journal of Engineering and Applied Sciences, Vol. 12, pp. 102-111, 2013.
4. A. Ansary Yar, M. Montazerian, H. Abdizadeh, and H. R. Baharvandi, Microstructure and mechanical properties of aluminium alloy matrix composite reinforced with nano-particle MgO, Journal of Alloys and Compounds, Vol. 484, No. 1-2, pp. 400-404, 2009.
5. Alhajeri, Saleh N., et al. "Microstructure and microhardness of an Al-6061 metal matrix composite processed by high-pressure torsion." Materials Characterization 118 (2016): 270-278.
6. B.S. Yigezu, M.M. Mahapatra and P.K. Jha, On modelling the abrasive characteristics of in situ Al-12%Si-TiC composites, Materials and Design, Vol. 50, pp. 277-284, 2013.
7. Baskaran, S., V. Anandakrishnan, and Muthukannan Duraiselvam. "Investigations on dry sliding wear behavior of in situ casted AA7075-TiC metal matrix composites by using Taguchi technique." Materials & Design 60 (2014): 184-192.
8. S. Rajech, A. Gopala Krishna, P. R.M. Raju and M. Duraiselvam, Statistical analysis of dry sliding wear behaviour of graphite reinforced aluminium MMCs, Procedia Materials Science, Vol. 6, pp. 1110-1120, 2014.
9. V. Ramakoteswara Rao, N. Ramanaiah, M.M.M. Sarkar, Mechanical and tribological properties of AA7075-TiC metal matrix composites under heat treated (T6) and cast conditions, Journal of Materials Research and Technology, Vol. 5, No. 4, pp. 377-383, 2016.
10. T. Babu Rao, An experimental investigation on mechanical and wear properties of Al7075/SiCp composites: effect of SiC content and particle size, Journal of Tribology, doi:10.1115/1.4037845 (In Press).
11. M. Vamsi Krishna, A.M. Xavior, An investigation on the mechanical properties of hybrid metal matrix composites, Procedia Engineering, Vol. 97, pp. 918-924, 2014.
12. N.G. Siddesh Kumar, V.M. Ravindranath and G.S. Shiva Shankar, Mechanical and wear behaviour of aluminium metal matrix hybrid composites, Procedia Material Science, Vol. 5, pp. 908-917, 2014.

13. S. J. James, K. Venkatesan, P. Kuppan and R. Ramanujam, Hybrid aluminium metal matrix composite reinforced with SiC and TiB₂, Procedia Engineering, Vol. 97, pp. 1018-1026, 2014.
14. P.S. Reddy, R. Kesavan and B.V. Ramnath, Investigation of mechanical properties of aluminium 6061-silicon carbide, boron carbide metal matrix composites, Silicon, https://doi.org/10.1007/s12633-016-9479-8, 2017.
15. Pradeep Sharma, Dinesh Khanduja and Satpal Sharma, Dry sliding wear investigation of Al6082/Gr metal matrix composites by response surface methodology, Journal of Materials Research and Technology, Vol. 5, No. 1, pp. 29-36, 2016.
16. S. Rajesh, A. Gopala Krishna, P.R.M. Raju and D. Muthukannan, Applications of grey-taguchi method for optimization of dry sliding wear properties of aluminium MMCs, Front. Mech. Eng. Vol. 7, No. 3, pp. 279-287, 2012.
17. S.T. Kumaran, M. Uthayakumar and S. Aravindan, Amalysis of dry sliding friction and wear behaviour of AA6351-SiC-B4C composites using grey relational analysis, Tribology – Materials, Surfaces & Interfaces, Vol. 8, No. 4, pp. 187-193, 2014.
18. P. Muthu, Optimization of dry sliding wear properties of aluminium MMCs using Grey Taguchi method, Journal of Advanced Microscopy Research, Vol. 12, No. 2, pp. 152-156, 2017.
19. Vignesh Kumar and R. Ramanujam, Experimental investigation and optimization of wear characteristics of metal matrix composites, International Journal of Innovative Science, Engineering & Technology, Vol. 2, No. 5, pp. 288-293, 2015.
20. Gangadhara Rao Ponugoti, Gopala Krishna Alluru & Pandu R. Vundavilli, Response surface methodology-based modelling of friction-wear behaviour of Al6061/9%Gr/WC MMCs and Its Optimization Using Fuzzy GRA, Transactions of the Indian Institute of Metals, doi: 10.1007/s12666-018-1377-x, 2018.
21. ASTM International. Standard test method for Brinell hardness of metallic materials. ASTM International; 2012.
22. ASTM E8 Test Methods for Tension Testing of Metallic Materials, Annual Book of ASTM Standards, vol. 03.01, 2003.
23. S. Dewangan, S. Gangopadhyay and C.K. Biswas, Multi-response optimization of surface integrity using grey-fuzzy logic-based hybrid approach, Engineering Science and Technology, an International Journal, Vol. 18, pp. 361-368, 2015.
24. D.K. Pratihari, Soft Computing: Fundamentals and Applications, Alpha Science International Limited, 2015.

AUTHORS PROFILE



Mr. P. Gangadhara Rao, is working as Associate Professor in Department of Mechanical Engineering Aditya College of Engineering and Technology Surampalem, Andhra Pradesh India-533437. He has published more than 10 research papers in indexed journals and conferences. He has 25 years of teaching experience (national and international). His area of interest in Optimization, Manufacturing. He is currently pursuing Ph.D. in Manufacturing at JNTUK. Kakinada.



Dr K. Meera Saheb, is currently Professor and Head of department, UCEKA, JNTUK Kakinada, A.P. He has published more than 30 research papers in indexed journals and attended/organized more than 30 conferences/workshops. He has 20 years of teaching experience and 15 years research experience. His area of interest in structural mechanics, vibrations, Optimization, and Manufacturing.



Dr. Pandu Ranga Vundavilli, working as Associate Professor, School of Mechanical Sciences, IIT Bhubaneswar. He got doctorate from IIT Kharagpur, India. He has more than 80 research publications. His specialized in the field of Robotics, Metal Matrix Composites, Manufacturing and Soft Computing tools. He has 20 years of teaching and research experience. He is a reviewer for a couple of journals.